

ElaStick: A Handheld Variable Stiffness Display for Rendering Dynamic Haptic Response of Flexible Object

Neung Ryu, Woojin Lee, Myung Jin Kim, Andrea Bianchi

Department of Industrial Design, KAIST

Daejeon, Republic of Korea

n.ryu@kaist.ac.kr, aerolane0302@gmail.com, dkmj@kaist.ac.kr, andrea@kaist.ac.kr

ABSTRACT

Haptic controllers have an important role in providing rich and immersive Virtual Reality (VR) experiences. While previous works have succeeded in creating handheld devices that simulate dynamic properties of rigid objects, such as weight, shape, and movement, recreating the behavior of flexible objects with different stiffness using ungrounded controllers remains an open challenge. In this paper we present ElaStick, a variable-stiffness controller that simulates the dynamic response resulting from shaking or swinging flexible virtual objects. This is achieved by dynamically changing the stiffness of four custom elastic tendons along a joint that effectively increase and reduce the overall stiffness of a perceived object in 2-DoF. We show that with the proposed mechanism, we can render stiffness with high precision and granularity in a continuous range between 10.8 and $71.5\text{Nmm}/^\circ$. We estimate the threshold of the human perception of stiffness with a just-noticeable difference (JND) study and investigate the levels of immersion, realism and enjoyment using a VR application.

Author Keywords

Haptics; Dynamic force response; Stiffness; Virtual Reality; Controller

CCS Concepts

•Human-centered computing → Human computer interaction (HCI);

INTRODUCTION

Haptic-force feedback can significantly increase the realism and enjoyment of Virtual Reality applications [16, 23]. Researchers from industry and academia have shown that the user perception of virtual worlds is greatly impacted by tangible proxies [20, 31] and haptics illusions [16, 28]. These, in tandem with a visual interface, contribute to altering the sensory perception of reality by tricking the senses. Following this approach, numerous researches present force-feedback

Permission to make digital or hard copies of all or part of this work for personal or classroom use is granted without fee provided that copies are not made or distributed for profit or commercial advantage and that copies bear this notice and the full citation on the first page. Copyrights for components of this work owned by others than the author(s) must be honored. Abstracting with credit is permitted. To copy otherwise, or republish, to post on servers or to redistribute to lists, requires prior specific permission and/or a fee. Request permissions from permissions@acm.org.

UIST'20, October 20–23, 2020, Minneapolis, MN, USA

© 2020 Copyright held by the owner/author(s). Publication rights licensed to ACM. ISBN 978-1-4503-6708-0/20/04...\$15.00

DOI: <https://doi.org/10.1145/3313831.XXXXXXX>

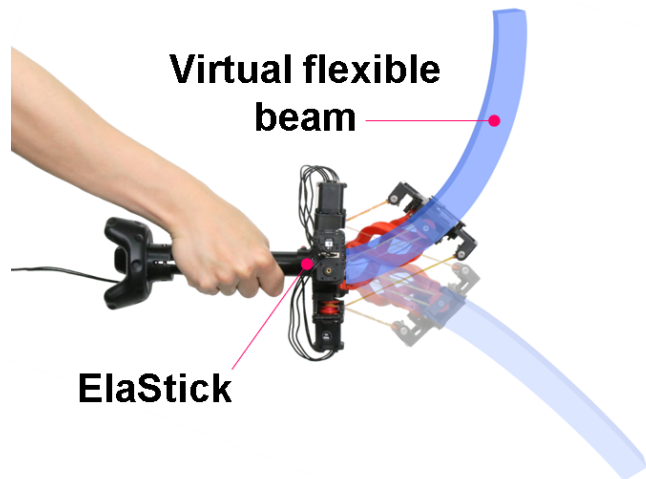


Figure 1. ElaStick allows to feel the dynamic response resulting from the movement of a virtual flexible object (e.g., a rubber beam).

controllers that render dynamic properties to simulate weights [5, 11], movement of masses [16, 28, 43], impacts [1, 40], and damped oscillations [39].

However, while previous works were able to recreate the illusion of different sizes and shapes of non-deformable objects [28, 31] or the movement of particles swirling in containers [26, 39], they did not focus on how flexible objects feels in the hand when swung. This includes how the center of mass shifts when the object is bent in multiple axes, and how the object physically reacts (i.e., dynamic response) when swung or shaken. Although some past research focused on stiffness displays capable of rendering deformable and bendable objects [10, 12, 36], they did not investigate how the users perceive the stiffness of these objects from their dynamic response. We therefore propose an ungrounded controller that renders this dynamic behavior of flexible objects, by changing the stiffness of the controller itself. With this setup, we can, for example, create the illusion of holding a beam made of rubber vs. a beam made of wood—the former feeling shaky and soft, and the latter feeling stiff and rigid (Figure 1). Similarly, we can also map the stiffness to other parameters of the object, such as its length and cross section, and therefore realistically render how it would respond in the real world.

This paper presents the following contributions. We present (1) a novel mechanism and its implementation through the development of the ElaStick controller prototype and a technical evaluation to determine its operational parameters; (2) a JND evaluation to estimate the human perception threshold of stiffness when freely swinging the ElaStick controller; (3) a study with a VR application in which users experience holding and swinging virtual beams of different stiffness and rate their perceived levels of realism, immersion, and enjoyment; (4) three applications that show extended usages of ElaStick, including continuous dynamic changes of stiffness and bi-manual control.

RELATED WORK

Ungrounded Force-Feedback in VR

Numerous handheld and wearable controllers have been proposed for rendering forces in VR applications and for achieving different illusions or haptic effects. These include the sensation of dynamic weights, moving center of masses, changes of shapes, and object oscillations.

Weight and impact: Lopes et al. [23] used electrical muscle stimulation (EMS) on the arm to create counter forces that the users perceived as repulsion and weight. Drag:on [44] has actuated folding fans attached to a game controller to modulate the air-resistance of the device when rotated or translated, creating the illusion of different weights and inertial properties of virtual objects. Thor’s Hammer [11] uses propellers to simulate pulling/pushing and gravitational forces. Similarly, Leviopole [27] uses the thrust from multirotors attached on each end of a pole to create the illusion of weights and resistance for various bimanual mid-air interactions. Very differently from these approaches, Grabity [5] achieves illusion of weight using asymmetric skin deformation, while Rietzler et al. [25] achieved it without applying any physical force or tactile feedback, but instead by using a software approach that deliberately creates perceivable tracking offsets that nudge users to lift their arm higher. Finally, researchers also explored several methods to generate impact forces: ElastImpact [38] and ElasticVR [40] stretch elastic bands and releases them to cause instant impacts on the arm and on a Head-Mounted Display (HMD), while Wind-blaster [17] uses the thrust of two propellers, mounted on each side of the wrist, to render impacts such as the recoil of a gun.

Varying center of mass and shapes: Dynamic changes in force applied to the controller result in perceivable changes in the center of mass and the illusion of changing shapes. Both Shifty [43] and TorqueBar [33] move a weight along a rail to render the effect of moving center of mass in one dimension. Aero-Plane [16] achieves the same effect on a 2D-plane without using moving masses, but by modulating the thrust of two fixed jet-propellers. Aero-plane can also create the illusion of objects with different shapes, by changing the intensity and the location of the force on the plane. A similar effect was achieved using mechanical moving parts for shape changing handheld controllers that vary their length [20] or fold in different planar configurations [28].

Shaking and oscillations: Several researchers explored the effect of shaking a device for realistically rendering the movement objects and oscillations of particles. Yamamoto et al [42] used shaking of a moving weight on a 1-DOF rail to simulate liquid and solid content inside a box. SWISH [26] extends this interaction in three dimensions, simulating the behavior of fluids inside a barrel-sized container. ElastOscillation [39] uses six extendable elastic bands to restrain the movement of a solid mass oscillating inside a cage. The degree in which the elastic bands are pulled affect the motion of the inner rigid body in 3-DOF, hence allowing users to perceive up to three distinct discreet levels of bounciness, such as differently sized food bouncing on a frying pan.

Our work differs from all the above by proposing a novel type of handheld stiffness display capable of rendering the dynamic response resulting from swinging flexible objects.

Stiffness Displays

Along with other haptic effects, researchers have also proposed several types of stiffness displays in the form of controllers that allow users to perceive the stiffness when grasping, bending, and poking objects or interacting with rigid bodies.

Grasping: CapstanCrunch [30] uses a friction-based capstan-plus-cord variable-resistance brake mechanism to generate varying resistive force that can simulate rigid and elastic objects grasped between the index finger and the thumb. Similar results were achieved by both Wolverine [6] and CLAW [7]. Wolverine simulates objects grasped between the thumb and three opposing fingers, while maintaining a low cost and lightweight hardware. CLAW uses a servo motor coupled with a force sensor and a voice coil actuator, not only to render the stiffness of different objects in the hand, but also to simulate touch and textures. PaCaPa [32], SqueezeBlock [9], and PuPoP [34] are all mechanical, actuated and pneumatic variations used to generate changes of pressure on the palm and fingers, hence creating the illusion of objects with different and varying sizes, as well as button-like feedback. Simon et al. [29] developed a mitten-shaped layer-jamming wearable haptic device that varies stiffness to simulate the grasping sensation of objects.

Bending: Tokuyama et al. [36] used bending and twisting motions through a PHANTOM haptic device to aid designers when bending and twisting 3D shapes. SPR1NG [10] uses a spring placed between two handles to bend and twist objects in virtual reality. PseudoBend [12] takes an alternative approach by rendering grain vibrations inside a rigid device to create the illusion of deformation from bending, stretching, and twisting when force or torque is applied with both hands. Bonanni et al. [3] developed a VR framework to bend and interact with slender one-dimensional objects through haptic devices.

Pushing: Stiffness displays can also render the deformation of objects under pressure. Free-form deformations, such as bending, can be rendered using a grounded device such as the Phantom [13] or DELTA [37] for manipulating virtual objects. Through these devices, users can perceive the haptic sensations of deforming free-form surfaces [15] with a pen-shaped probe. Other applications allow interacting with and experiencing

the elasticity of objects with different stiffness [13] through two-finger interaction, and poking virtual organs such as a liver with a probe [37].

Interaction with rigid bodies: Other stiffness displays focus on supporting the interaction with rigid or constrained bodies. Haptic Links [31] uses the locking and releasing mechanisms of three different configurations of linkages between a pair of controllers. The device supports the haptic rendering of a variety of bi-manual objects and interactions. Elastic-Arm [1] and HapticSphere [41] use a body-mounted elastic armature linking the wearer’s hand to the shoulder or HMD that causes a progressive resistance force to be perceived when extending the arm and provides haptic cues about the surrounding environment. Follmer et al. [8] and jamSheets [24] presented explorations of particle jamming and layer jamming techniques that enable malleable and thin input interfaces of variable stiffness, respectively.

Our work differs from the other stiffness displays presented in this section by introducing a novel ungrounded handheld device capable of simulating the inertial forces generated by bending bodies when shaken.

THE ELASTICK SYSTEM

ElaStick is a haptic handheld device capable of simulating the mechanical impedance that a flexible object, such as a beam, generates when abruptly swung or shaken. This dynamic behavior is usually perceived through a combination of mass-shifting, due to the object bending, together with the delayed response and vibrations caused by the object resuming its original state. The intensity of these forces depends on the strength, direction and acceleration of the motion and the physical properties of the material—the size and shape of the object and the stiffness of its material. For example, shaking an elastic/long/thin beam produces a larger dynamic response than an equivalent object that is rigid/short/thick. By changing the stiffness of a 2-DOF joint, ElaStick is capable of rendering the effect (i.e., the mechanical impedance) of objects with different elasticity properties (material, shape, and size).

Mechanism

By applying an orthogonal force (F_1) to the tip of a rectangular beam in relax state, the beam flexes in proportion to the moment $F \times L$ (Figure 2). As described in Equation 1, the

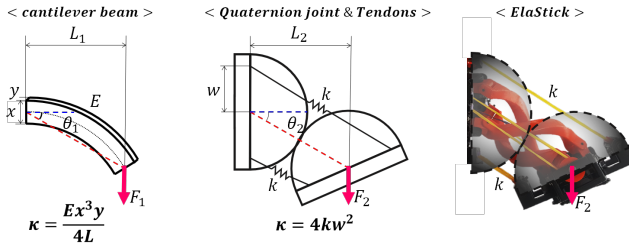


Figure 2. Equivalent diagram of rotational stiffness for a rectangular beam and ElaStick’s mechanism. On the right, the quaternion joint mechanism, which summates two spheres rolling on each other reducing slip.

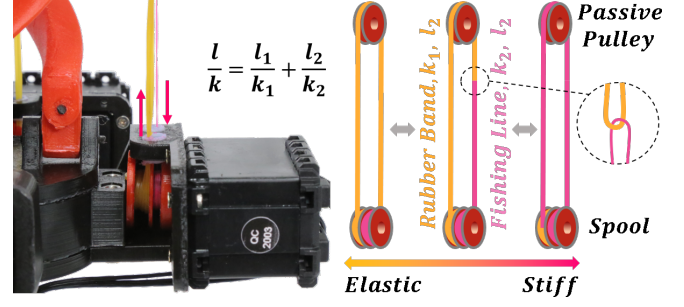


Figure 3. The mechanism to control the tendons and the formula to compute the tendon’s stiffness k given the stiffness of an elastic k_1 and inelastic k_2 wire of lengths l_1 and l_2 .

amount of bending (θ) is inversely proportional to the rotational stiffness of the beam (κ) — the stiffer the bar, the less it bends.

$$F \times L = \kappa \theta \quad (1)$$

The rotational stiffness κ is defined as a function of the beam’s cross-section shape and length (x , y , and L) and its material stiffness, described using Young’s modulus (E). ElaStick is based on this model, but instead of relying on the stiffness of the beam itself, it uses a rigid joint in combination with a pair of elastic tendons for each axes. We derived the new rotational stiffness of the device as $\kappa = 4kw^2$, where k is the stiffness of the tendons and w is the distance between the tendons and the center of the base. Given the same input moment ($F_1 \times L_1 = F_2 \times L_2$), ElaStick can then render the same bending behavior of the cantilever beam ($\theta_2 = \theta_1$) by simply controlling k .

Each tendon has a size of 20cm and it is made from a longer string of two wires of different materials connected in series — an inelastic fishing wire and a natural rubber band are looped through each other to avoid the bump resulting from a knot (Figure 3). Both ends of the string are attached to a spool and loop through a pulley, forming a tendon. By rotating the spool, one end of the wire is wound around the spool, while the other end is unwound. This novel mechanism allows to control the proportion of elastic and inelastic materials of the string that makes up a tendon. Specifically, by changing this proportion (e.g., the length), we can vary the tendons’ overall stiffness (k). The equation describing the cumulative stiffness is shown in Figure 3.



Figure 4. The quaternion joint achieves 2-DOF wide rotational angle.

Because a single tendon can only provide tensile force and not compressive force, we designed the tendons to be placed symmetrically about the center to provide antagonistic stiffness.

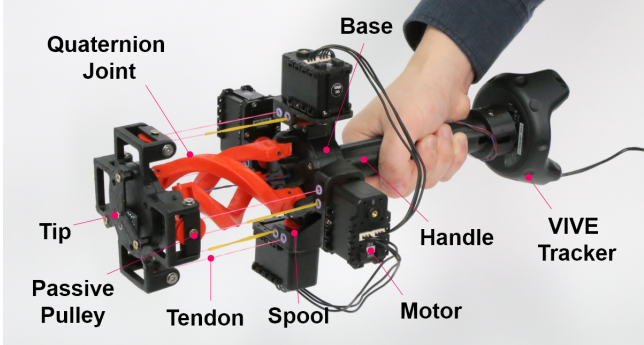


Figure 5. ElaStick overview and its parts.

To maintain a reliable antagonistic behavior the tendons must remain parallel, which is not possible with traditional ball-socket joints. Therefore, we resorted to a quaternion joint [19], which allows to place tendons in parallel and behaves such that the extension on one side results in a symmetric compression on the other. The quaternion joint and its range of movements (± 45 degrees/axis) is shown in Figure 4.

Implementation

ElaStick is made of a quaternion joint, two pairs of tendons with a stiffness changing mechanism, a handle with an input button, and a VIVE tracker placed at the rear end of the handle (Figure 5). The quaternion joint has a height of 122 mm, and a diameter of 60mm, which maintain the tip of the joint within an operation radius of 100mm. The tip, mounted on one end of the joint, can rotate ± 45 degrees in two axes, hence remaining tangential to the inner sphere's surface. Four servo motors (Dynamixel MX-12W, Weight: 54.60g, Voltage: 12V, RPM: 460, Signal latency : ≤ 0.5 ms) are mounted on the base and are used to wind and unwind the spools. Motors can be activated simultaneously or selectively. It takes about 1 second for the tendon to transition entirely from one material to the other. In the neutral state, the rubber band that composes tendons is approximately 200% stretched, and its elongation varies from approximately 100% to 300% depending on the movement of the device. In this range of stretching, the natural rubber can endure up to 10^6 cycles before breaking [4]. Finally, the parts where the tendons slide through are coated with Teflon to prevent frictional wear.

A push-button, which connects to an external Arduino Mega, is mounted on the cylindrical handle for input control (handle diameter: 26mm, length: 150mm). The overall structure was 3D printed with PolyLactic Acid (PLA). It measures 170mm \times 170mm \times 375mm and weights 596g. The firmware for motor control is written in C++ and runs on an Arduino Mega with the Dynamixel Shield extension. A software running on a PC communicates to the Arduino via serial the desired stiffness levels, and the Arduino moves the motors accordingly.

TECHNICAL EVALUATION

We conducted a technical evaluation to determine ElaStick's mechanical characteristics and structural behavior. The evaluation was designed to determine the following properties: (1) the range of stiffness that can be rendered using ElaStick, (2)

the numerical relationship between stiffness of the device and the rotations of the spools, and (3) the equivalent inertia and damping coefficient of the device.

Stiffness evaluation

To measure the stiffness of the device, we followed a common method found in literature [22]. We positioned ElaStick horizontally on a table and tightly fixed it with a clamp by the handle (Figure 6). After attaching or removing loads with different weight to the tip of the device, we measured the resulting bending of the joint using a gyro sensor placed on the device's tip. Specifically, we used six loads of 50g, for a total of 300g, attached to the tip using an inelastic fishing wire. For the bending measurements, we collected and averaged 10 samples at 100Hz with an MPU6050 gyro sensor connected to an Arduino Mega.

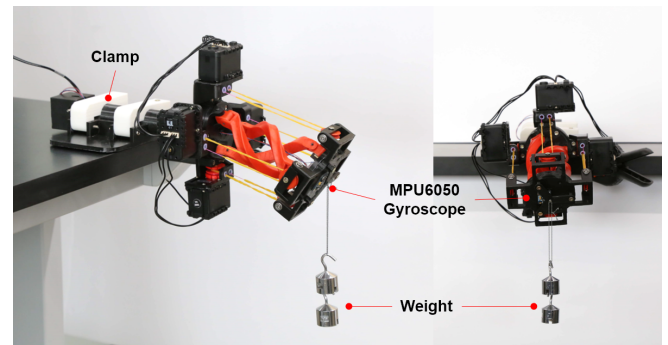


Figure 6. Stiffness evaluation setup.

We repeated this process by varying the stiffness of the tendons through the rotation of the spools. Specifically, we considered the range between 0 and 7 rotations (the maximum physically supported) with increments of 0.2 rotations. This resulted in 36 distinct tendons configurations, by 12 weights (down from 300g to 0g, and then back up), by 3 times (repeated measures). In total we collected 1296 data points.

From the collected data we obtained 36 moment-angle curves, representing the stiffness values in the range between 0 and 7 rotations at intervals of 0.2. The graphs in Figure 7 show six example of these curves, chosen with constant intervals of 1.4 rotations. These graphs reveal a significant hysteretic behavior. For each of the 36 curves we then computed the secant angular stiffness (i.e. the slope of the red lines in Figure 7) using Equation 2, where $M_{max/min}$ is the maximum and minimum

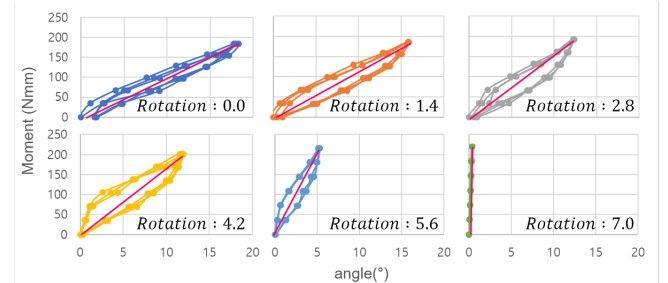


Figure 7. Examples of moment-angle curves showing hysteresis.

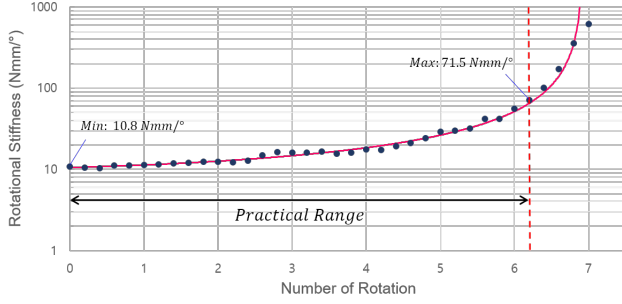


Figure 8. Rotational stiffness over the range 0-7 rotations and practical stiffness range. The prediction model is based on the quadratic regression shown in red.

moment produced by weights and $\theta_{max/min}$ is the deflected angle.

$$\kappa = \frac{M_{max} - M_{min}}{\theta_{max} - \theta_{min}} \quad (2)$$

These computed stiffness values are plotted over the full range of rotations in Figure 8. The range spans between a minimum of 10.8Nmm/° and a maximum of 616.5Nmm/° , which physically corresponds to the stiffness of a beam made respectively of rubber or wood, with a cross-section of $30\text{mm} \times 30\text{mm}$ and length of 300mm . However, because of the low vertical resolution beyond 71.5Nmm/° (6.2 rotations), we limited the maximum stiffness to this value (i.e., the stiffness of high-density polyethylene). Therefore, subsequent studies and applications presented in this paper use a range between 10.8Nmm/° and 71.5Nmm/° , reserving the absolute maximum stiffness value only to completely lock one of the axis (e.g., rigid object).

Finally, we analyzed the device's overall behavior. This is necessary to generalize the mapping between stiffness and rotation. We conducted a linear and a quadratic regression using the inverse stiffness computed from the points in Figure 8. Linear and quadratic regression resulted respectively in $R^2 = 0.9628$ and $R^2 = 0.9877$. The quadratic regression led to more reliable fitting. We speculate that this effect is caused by mechanical imperfections: when the tendons are wound onto a spool they stack and consequently increase or reduce the radius of the spool. This affects the linear relationship between number of rotations and the stiffness. Therefore, in agreement with our regression results, we adopted a quadratic function to predict and control the stiffness of ElaStick.

Step-Response Evaluation

The second technical evaluation aims to determine the system's dynamic response by observing the step-response. This evaluation is necessary to determine the inertia and damping coefficient, which we will eventually use for simulating flexible objects in VR applications.

To collect the step-responses we followed this method. As above, ElaStick was fixed horizontally to a table, with a gyro sensor (MPU6050) mounted on the tip. We pulled the device's tip downward and then immediately released it, so to generate a step input. We repeated this process five times for

	f_d (Hz)	f_n (Hz)	I_{eq}^* ($\text{g}\cdot\text{m}^2$)	OS%	ζ^*
κ	5.47	5.53	0.570	62.5	0.148
2κ	7.81	7.95	0.564	54.9	0.187
4κ	11.09	11.21	0.559	66.8	0.128

Table 1. Summary of result for step-response. I_{eq} and ζ show no statistically significant differences (at significance level $\alpha = 0.05$).

three representative stiffness: 12.5 , 25.0 , and 50.0 Nmm/° — which from now on we will refer to as κ , 2κ , 4κ . These values were chosen to be multiples and to cover as much as possible of the practical range. The tip's oscillations were captured by the gyro sensor and are graphed in Figure 9. We then conducted a fast Fourier transform to derive the damped frequency (f_d) for each stiffness condition, and derived the percentage overshoot (OS%) to estimate the damping ratio (ζ). Natural frequency (f_n) and equivalent inertia (I_{eq}) were calculated using the equations in literature [21].

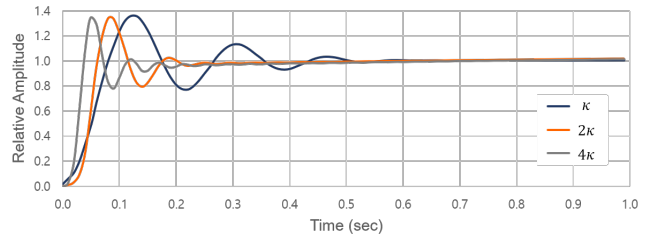


Figure 9. Step-response of ElaStick for three reference stiffness values.

All results are shown in Table 1. The computed equivalent inertia (I_{eq}) and the damping ratios (ζ) are respectively 0.564gm^2 (SD: 0.071) and 0.16 (SD: 0.04). Finally, we conducted a one-way ANOVA ($\alpha = 0.05$) for the equivalent inertia values and damping ratios, which resulted in no significant differences across the three reference stiffness values: $F_{2,12} = 0.02$, $p = 0.98$ for I_{eq} , and $F_{2,12} = 2.96$, $p = 0.09$ for ζ . These results confirms that changes of stiffness rendered by ElaStick do not affect other parameters such as inertia and damping.

Technical Evaluation summary

In summary, through these technical evaluations we are able to determine that ElaStick's rotational stiffness follows a quadratic curve, it is capable to generate and control stiffness in its practical range 10.8Nmm/° and 71.5Nmm/° (0 rotations to 6.2 rotations) and provides a maximum stiffness of 616.5Nmm/° (7 rotations). Also we found that the inertia and the damping ratio are independent from the stiffness control and they have constant value of 0.564gm^2 and ratio of 0.16.

USER STUDY 1: JND ESTIMATION

To measure the users' perception of stiffness with varying elasticity coefficients, we performed a study of Just-Noticeable Differences (JND) [18]. While prior work reported JND results about the ability of human subjects to discern weights through the action of shaking them [42], and about the discrimination of both passive and active natural frequency for oscillating objects [14], there is no literature describing the human perception of varying stiffness for flexible object held

and shaken in the hand. Our JND study is motivated by this absence.

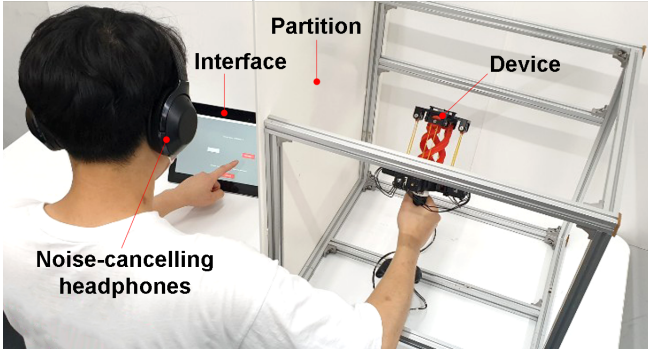


Figure 10. JND study setup.

Eight participants (two female) aged 19-29 (M: 24.25, SD: 3.37) were recruited for the study. All participants but one were right-handed, and none had arm injuries or impairments. All participants were students from our institution at the time of the study, and were compensated with 10 USD in local currency.

Study setup

Our method closely mirrors that presented in prior work [35], which investigated the perception of haptic compliance with active input from users. While prior work measured perceived stiffness of objects that were sequentially presented to the users and needed to be *actively* squeezed for discrimination, in our work we use ElaStick to sequentially present two different levels of stiffness that can be perceived by *actively* shaking or freely swinging the device. Participants then indicate, for each pair of stimuli which one was perceived stiffer, using a touch screen with a graphical computer interface. This constitutes a single trial.

Following previous work [35], we built blocks of trials in this method. We selected three reference stiffness levels S (of values κ , 2κ , 4κ , derived from the technical evaluation) and six variations ΔS ($\pm 5\%$, $\pm 10\%$, and $\pm 15\%$ of S). This means that for each reference stiffness, we generated six testing stimuli ($S + \Delta S$). The result is a block of 12 trials of reference-testing stimuli, which accounts for all the combinations and orders.

For this study, each participant was presented with 180 trials (3 reference stiffness \times 5 blocks \times 12 trials), with trials randomized within each block. The first block was considered as a training session and corresponding trials were excluded from the analysis. Throughout the experiment, participants sat comfortably in front of a computer, while holding ElaStick with their dominant hand. A physical partition and noise-canceling headphones playing white-noise were used to block visual and auditory cues. There were no limitations on the amount of time per trial, but we enforced a mandatory 5 minute break between blocks. Participants were also encouraged to take rests at any point during the experiment. The software for collecting the data was developed in Java. It allows to control ElaStick via serial communication.

Results

The resulting data represent the number of times that a test stimulus was felt to be stiffer than the reference. This is a function of the difference of stiffness between the test and the reference. We then fit this data in a cumulative Gaussian curve, as in [35]. The width of the cumulative Gaussian corresponds to the probability of 84% that a testing force was perceived stiffer than the reference stimulus (discrimination threshold, or JND). This result is highlighted in Figure 11.

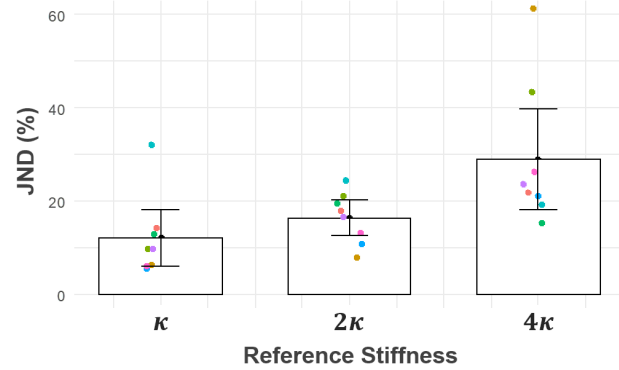


Figure 11. Result of the JND study, for each of the reference stiffness values. The bar chart indicates the average value of JND and the error-bar represents a 95% of confidence interval. Each colored points indicates different participants.

We report the average JND as the ratio $\Delta S/S$, for each of the reference stiffness: 11.99% (SD: 8.66) for κ , 16.33% (SD: 5.56) for 2κ , and 28.98% (SD: 15.57) for 4κ . Overall, our data shows a trend for which JND grows with the increase of the reference stiffness. These results indicate that our device can provide at least eight distinguishable stiffness levels within the considered practical range, if we use a JND of 28.98%, the most conservative of the measurements reported.

USER STUDY 2: USER EXPERIENCE

We conducted a second study to observe how users rated ElaStick's haptic compliance for immersion, realism and enjoyment. Eight participants (five female), aged 20-38 (M: 25.88, SD: 5.39) volunteered for the study. All participants were right-handed, none reported hand/arm injuries or impairment. All participants were students in our institution at the time of the study, and were compensated with 5 USD in local currency.

Using Unity 3D and C#, we built a VR application that tracks the motion of the ElaStick controller in real-time and maps it to the movements of a rectangular virtual beam that bends according to different levels of stiffness. This bending effect was achieved in software by modeling the beam using a configurable joint set with the values of inertia, damping ratio and stiffness that we measured in the technical evaluation. To account for the differences in shape and size of the virtual beam and the ElaStick controller, we made the assumptions that the tip of the virtual beam and that of ElaStick have the same angular position and velocity, and then computed the beam's curvature using Euler-Bernoulli beam theory [2].

For the experiment we constructed virtual beams with three different lengths (*Short*=37.5cm, *Medium*=75cm, *Long*=150cm)

and three different cross sections (*Square* = 30×30mm, *Horizontal* = 20×100mm, and *Vertical* = 100×20mm) for a total of nine combinations of lengths and shapes (Figure 12). These were mapped in hardware to three degrees of stiffness (κ , 2κ , 4κ), such that each beam configuration had the exact stiffness of an equivalently sized silicon rubber beam in the real world. Finally, while for the *Square* cross section the beam could be moved in two axes with the same level of stiffness, for the other shapes the longer axis was considered completely stiff (616.5Nmm/° corresponding to 7 rotations, maximum possible).

The experiment followed a within-subject design setup with balanced conditions. As in prior work [16, 23], for each of the nine configurations of the beam described above, the participants experienced and rated the realism, immersion and enjoyment in the two conditions—*visual* vs. *visual + haptic*. In the *visual* condition users swung and shook the beam using ElaStick set with maximum stiffness and hence no haptic feedback. In the *visual + haptic* condition, users had both the haptic and the visual feedback.

The physical setup of the study and procedure was identical between the two conditions. Participants stood in a room wearing a VIVE HMD and noise-canceling headphones playing white noise, and holding the ElaStick controller in their dominant hand. They were given then the chance to experience unconstrained movements of the controller for at least 1 minute for each configuration. Configurations were presented in a fixed order (as in Figure 12, from left to right). As in prior work [16, 23], after each condition the participants filled a questionnaire with 7-point Likert scale questions about immersion, realism and enjoyment. We also conducted a post-hoc interview to gather qualitative findings about the overall experience and various feedback.

Results

The overall scores per conditions is presented in Figure 13. Participants rated the *visual + haptic* condition with higher scores than the *visual* condition. A Wilcoxon signed rank test reveals statistically significant differences between conditions, for all the measured variables: immersion ($Z = -2.264$, $p = 0.024$), realism ($Z = -2.214$, $p = 0.027$), and enjoyment ($Z = -2.050$, $p = 0.040$).

The interviews were conducted in the local language and transcribed and analyzed by one researcher using open and axial coding methods to extract qualitative comments. All users agreed that the haptic experience was the most engaging and

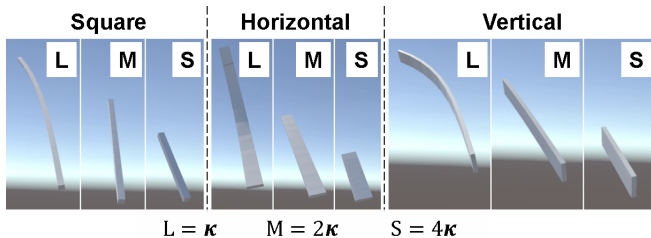


Figure 12. All the configurations considered for the study.

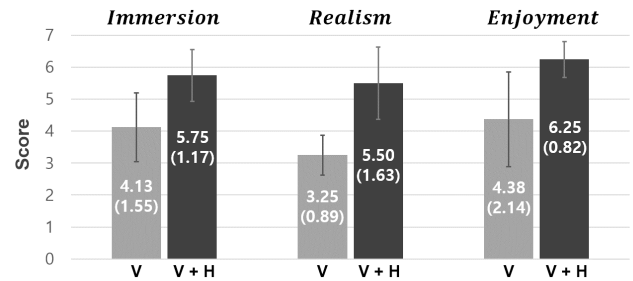


Figure 13. Plot of average values with standard error bars. The user ratings shows consistent significant differences between *visual* (V) and *visual + haptic* (V+H) conditions.

immersive, with participants commenting that "it felt like a real thing (P6)" and "natural (P1)". In stark comparison, the visual-only experience was reported to feel "awkward (P2)", "fake (P7)", and even "boring (P2)". P7 elaborated that the reason why s/he felt this way was because the beam in the virtual space "moved [bent] more than the effort put in".

Participants were mostly surprised by the rendering of different lengths and cross-sections, commenting that they "felt dramatic difference [...] when length changed (P2)" and that they could "definitely feel the asymmetry of the flat beam (P3)". We could also observe increased enjoyment, with some users commenting that "the flat shape with both visual and haptic feedback was my favorite! It was really fun (P2)".

However, users pointed out some limitations of the system. Specifically, P6 mentioned that "the realism decreased because the device was heavy" and P1 reckoned that "it was awkward that the shape of the [physical] handle was different from the one in VR". P1 commented that because of the low frame rate and visual latency, "...it had an unreal feeling." Similarly, because of visual artifacts generated by deformable surfaces, P6 mentioned "it reduced the immersion," and caused to "interact[ed] with the device less actively." Finally, participants suggested some possible applications of ElaStick for VR experiences, including fishing, mixing fluids, games and acoustic effects.

APPLICATIONS

To show various uses of ElaStick beyond the simple example of a flexible beam used in the user evaluation, we developed three additional applications. Overall these applications aim to demonstrate that ElaStick can control multiple degrees of stiffness in two independent axes dynamically over time. We also include an application requiring bi-manual control, that shows the potential of applying ElaStick's mechanism to a different form-factor.

The Fencing application (Figure 14) best demonstrates the device's ability to render the varying stiffness of handheld virtual objects using two independent axes. The user can experience fencing with three weapons—the foil, the sabre, and the epee—each uniquely characterized by specific stiffness responses. The foil has the most flexible blade, thin with a rectangular cross-section that allows flexion in any axis (11.0Nmm/° stiffness). The sabre is shorter and stiffer with

a Y-shaped cross section that makes the blade stiffer across the vertical axis (20.0Nmm° and 70.0Nmm° across the x and y axes). Finally, the epee is the stiffest with a triangular cross section that makes the blade uniformly rigid (70Nmm° stiffness).

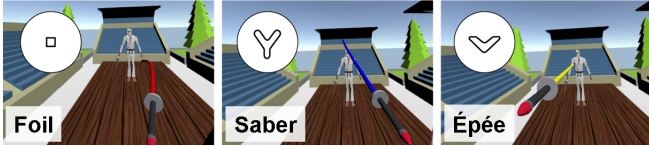


Figure 14. Using three fencing weapons with different cross sections and stiffness (identified by users using different colors).

Dynamic stiffness can be used to recreate changing properties of materials such as their state (e.g., solidifying, hardening/freezing, softening/melting) or shapes (e.g., elongating, shortening). This can be useful for generating applications that require high realism, such as industrial training or more immerse games. For example, we created an application for increasing the realism of cooking in VR, as seen in the Whipping Batter application (Figure 15). In this application the user experiences whipping a cream in a bowl. While initially the cream is liquid and the batter is perceived flexible in any direction, with time passing and the cream becoming whipped, the batter consequently becomes stiffer.

In the last application we demonstrate that ElaStick's form-factor can be modified to support handheld interactions beyond shaking with one hand. In the Power Twister application an additional physical handle is attached to the tip of ElaStick, turning the device into a bi-manual controller for physical exercises in a virtual gym. By bending the device, the user experiences different degrees of stiffness, similarly to the weight adjustments of a power twister.

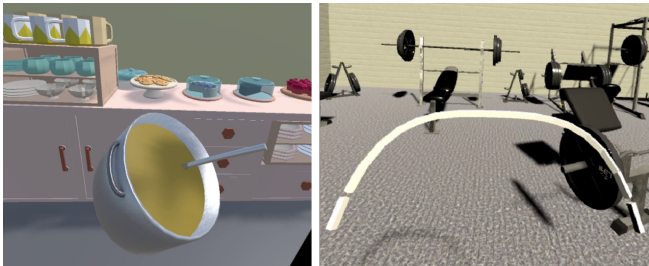


Figure 15. Whipping batter (left) and power twister bar (right).

LIMITATIONS AND CONCLUSIONS

This paper presents numerous areas of improvements. The mechanical model on which ElaStick is based on is a convenient simplification that holds true for bending angles smaller than 30 degrees. Although we pushed this device further than the limit (45 degrees), users did not report loss of realism. Furthermore, while in the real world a flexible beam would have infinite degrees of freedom, ElaStick is only capable of rendering 1 DOF movement per rotational axis. However, through our current studies, we did not notice any decreased realism or immersion.

Some of the participants commented that the heaviness of ElaStick disturbed the haptic experience. The weight of the prototype can be reduced using smaller motors or reducing the size of the joint structure. An alternative approach is to take advantage of the device's weight for generating stronger force feedback. To achieve this, we could reconfigure the mass distribution, by relocating the motors from the base to the tip of the device. Finally, we see an opportunity to improve our tracking mechanism with a closed-loop synchronization, and to perform users tests simultaneously using multiple stiffness levels for different axes.

In conclusion, in this paper we introduced ElaStick, a novel handheld VR controller that allows to feel the dynamic response of flexible moving objects in virtual reality through dynamic changes of stiffness. We presented a model for changing stiffness of a 2-DOF quaternion joint using tendons of varying stiffness. We then presented the first attempt to measure the human perception threshold for the dynamic response of flexible objects with an ungrounded device (JND study). In a subsequent study, we assessed the levels of realism, immersion and enjoyment of a VR application, which uses the ElaStick controller to simulate flexible beams of various shape and size. Finally, based on the users' feedback, we created few example applications that explore the design space of this novel stiffness display.

ACKNOWLEDGEMENTS

This research was supported by the MSIT (Ministry of Science and ICT), Korea, under the Grand Information Technology Research Center support program (IITP-2020-2015-0-00742) supervised by the IITP (Institute for Information & communications Technology Planning & Evaluation).

REFERENCES

- [1] Merwan Achibet, Adrien Girard, Anthony Talvas, Maud Marchal, and Anatole Lécuyer. 2015. Elastic-Arm: Human-scale passive haptic feedback for augmenting interaction and perception in virtual environments. In *2015 IEEE Virtual Reality (VR)*. IEEE, 63–68.
- [2] R.R. Archer, S.H. Crandall, N.C. Dahl, T.J. Lardner, and M.S. Sivakumar. 2012. *An Introduction to Mechanics of Solids*. Tata McGraw-Hill Education Private Limited. <https://books.google.co.kr/books?id=VczjAzm7vAC>
- [3] Ugo Bonanni, Petr Kmoch, and Nadia Magnenat-Thalmann. 2009. Haptic Interaction with One-Dimensional Structures. In *Proceedings of the 16th ACM Symposium on Virtual Reality Software and Technology (VRST '09)*. Association for Computing Machinery, New York, NY, USA, 75–78. DOI: <http://dx.doi.org/10.1145/1643928.1643946>
- [4] SM Cadwell, RA Merrill, CM Sloman, and FL Yost. 1940. Dynamic fatigue life of rubber. *Rubber Chemistry and Technology* 13, 2 (1940), 304–315.
- [5] Inrak Choi, Heather Culbertson, Mark R. Miller, Alex Olwal, and Sean Follmer. 2017. Grabity: A Wearable Haptic Interface for Simulating Weight and Grasping in Virtual Reality. In *Proceedings of the 30th Annual ACM*

- Symposium on User Interface Software and Technology (UIST '17)*. Association for Computing Machinery, New York, NY, USA, 119–130. DOI: <http://dx.doi.org/10.1145/3126594.3126599>
- [6] I. Choi, E. W. Hawkes, D. L. Christensen, C. J. Ploch, and S. Follmer. 2016. Wolverine: A wearable haptic interface for grasping in virtual reality. In *2016 IEEE/RSJ International Conference on Intelligent Robots and Systems (IROS)*. 986–993.
 - [7] Inrak Choi, Eyal Ofek, Hrvoje Benko, Mike Sinclair, and Christian Holz. 2018. Claw: A multifunctional handheld haptic controller for grasping, touching, and triggering in virtual reality. In *Proceedings of the 2018 CHI Conference on Human Factors in Computing Systems*. 1–13.
 - [8] Sean Follmer, Daniel Leithinger, Alex Olwal, Nadia Cheng, and Hiroshi Ishii. 2012. Jamming User Interfaces: Programmable Particle Stiffness and Sensing for Malleable and Shape-Changing Devices. In *Proceedings of the 25th Annual ACM Symposium on User Interface Software and Technology (UIST '12)*. Association for Computing Machinery, New York, NY, USA, 519–528. DOI: <http://dx.doi.org/10.1145/2380116.2380181>
 - [9] Sidhant Gupta, Tim Campbell, Jeffrey R Hightower, and Shwetak N Patel. 2010. SqueezeBlock: using virtual springs in mobile devices for eyes-free interaction. In *Proceedings of the 23rd annual ACM symposium on User interface software and technology*. 101–104.
 - [10] Tomás Henriques. 2019. SPR1NG Controller: An Interface for Kinesthetic Spatial Manipulation. In *2019 IEEE 7th International Conference on Serious Games and Applications for Health (SeGAH)*. IEEE, 1–5.
 - [11] Seongkook Heo, Christina Chung, Geohyuk Lee, and Daniel Wigdor. 2018. Thor's hammer: An ungrounded force feedback device utilizing propeller-induced propulsive force. In *Proceedings of the 2018 CHI Conference on Human Factors in Computing Systems*. 1–11.
 - [12] Seongkook Heo, Jaeyeon Lee, and Daniel Wigdor. 2019. PseudoBend: Producing Haptic Illusions of Stretching, Bending, and Twisting Using Grain Vibrations. In *Proceedings of the 32nd Annual ACM Symposium on User Interface Software and Technology*. 803–813.
 - [13] Koichi Hirota and Toyohisa Kaneko. 2001. Haptic representation of elastic objects. *Presence: Teleoperators & Virtual Environments* 10, 5 (2001), 525–536.
 - [14] Ali Israr, Yanfang Li, Volkan Patoglu, and Marcia K O'Malley. 2008. Passive and active discrimination of natural frequency of virtual dynamic systems. *IEEE transactions on haptics* 2, 1 (2008), 40–51.
 - [15] Hiroo Iwata. 1993. Pen-based haptic virtual environment. In *Proceedings of IEEE Virtual Reality Annual International Symposium*. IEEE, 287–292.
 - [16] Seungwoo Je, Myung Jin Kim, Woojin Lee, Byungjoo Lee, Xing-Dong Yang, Pedro Lopes, and Andrea Bianchi. 2019. Aero-plane: A Handheld Force-Feedback Device that Renders Weight Motion Illusion on a Virtual 2D Plane. In *Proceedings of the 32nd Annual ACM Symposium on User Interface Software and Technology*. 763–775.
 - [17] Seungwoo Je, Hyelin Lee, Myung Jin Kim, and Andrea Bianchi. 2018. Wind-Blaster: A Wearable Propeller-Based Prototype That Provides Ungrounded Force-Feedback. In *ACM SIGGRAPH 2018 Emerging Technologies (SIGGRAPH '18)*. Association for Computing Machinery, New York, NY, USA, Article Article 23, 2 pages. DOI: <http://dx.doi.org/10.1145/3214907.3214915>
 - [18] Lynette A Jones and Hong Z Tan. 2012. Application of psychophysical techniques to haptic research. *IEEE transactions on haptics* 6, 3 (2012), 268–284.
 - [19] Yong-Jae Kim, Jong-In Kim, and Wooseok Jang. 2018. Quaternion Joint: Dexterous 3-DOF Joint representing quaternion motion for high-speed safe interaction. In *2018 IEEE/RSJ International Conference on Intelligent Robots and Systems (IROS)*. IEEE, 935–942.
 - [20] Andrey Krekhov, Katharina Emmerich, Philipp Bergmann, Sebastian Cmentowski, and Jens Krüger. 2017. Self-transforming controllers for virtual reality first person SHOOTERS. In *Proceedings of the Annual Symposium on Computer-Human Interaction in Play*. 517–529.
 - [21] Erwin Kreyszig. 1983. *Advanced engineering mathematics*. Fifth edition. New York : Wiley, [1983] ©1983. <https://search.library.wisc.edu/catalog/999526345802121>
 - [22] Sebastian Linß, Philipp Schorr, and Lena Zentner. 2017. General design equations for the rotational stiffness, maximal angular deflection and rotational precision of various notch flexure hinges. *Mechanical Sciences* 8, 1 (2017), 29.
 - [23] Pedro Lopes, Sijing You, Lung-Pan Cheng, Sebastian Marwecki, and Patrick Baudisch. 2017. Providing Haptics to Walls & Heavy Objects in Virtual Reality by Means of Electrical Muscle Stimulation. In *Proceedings of the 2017 CHI Conference on Human Factors in Computing Systems (CHI '17)*. Association for Computing Machinery, New York, NY, USA, 1471–1482. DOI: <http://dx.doi.org/10.1145/3025453.3025600>
 - [24] Jifei Ou, Lining Yao, Daniel Tauber, Jürgen Steimle, Ryuma Niiyama, and Hiroshi Ishii. 2014. JamSheets: Thin Interfaces with Tunable Stiffness Enabled by Layer Jamming. In *Proceedings of the 8th International Conference on Tangible, Embedded and Embodied Interaction (TEI '14)*. Association for Computing Machinery, New York, NY, USA, 65–72. DOI: <http://dx.doi.org/10.1145/2540930.2540971>

- [25] Michael Rietzler, Florian Geiselhart, Jan Gugenheimer, and Enrico Rukzio. 2018. Breaking the Tracking: Enabling Weight Perception Using Perceivable Tracking Offsets. In *Proceedings of the 2018 CHI Conference on Human Factors in Computing Systems (CHI '18)*. Association for Computing Machinery, New York, NY, USA, Article Paper 128, 12 pages. DOI: <http://dx.doi.org/10.1145/3173574.3173702>
- [26] Shahabedin Sagheb, Frank Wencheng Liu, Alireza Bahremand, Assegid Kidane, and Robert LiKamWa. 2019. SWISH: A Shifting-Weight Interface of Simulated Hydrodynamics for Haptic Perception of Virtual Fluid Vessels. In *Proceedings of the 32nd Annual ACM Symposium on User Interface Software and Technology*. 751–761.
- [27] Tomoya Sasaki, Richard Sahala Hartanto, Kao-Hua Liu, Keitarou Tsuchiya, Atsushi Hiyama, and Masahiko Inami. 2018. Leviopole: Mid-Air Haptic Interactions Using Multirotor. In *ACM SIGGRAPH 2018 Emerging Technologies (SIGGRAPH '18)*. Association for Computing Machinery, New York, NY, USA, Article Article 12, 2 pages. DOI: <http://dx.doi.org/10.1145/3214907.3214913>
- [28] Jotaro Shigeyama, Takeru Hashimoto, Shigeo Yoshida, Takuji Narumi, Tomohiro Tanikawa, and Michitaka Hirose. 2019. Transcalibur: A Weight Shifting Virtual Reality Controller for 2D Shape Rendering based on Computational Perception Model. In *Proceedings of the 2019 CHI Conference on Human Factors in Computing Systems*. 1–11.
- [29] Timothy M. Simon, Ross T. Smith, and Bruce H. Thomas. 2014. Wearable Jamming Mitten for Virtual Environment Haptics. In *Proceedings of the 2014 ACM International Symposium on Wearable Computers (ISWC '14)*. Association for Computing Machinery, New York, NY, USA, 67–70. DOI: <http://dx.doi.org/10.1145/2634317.2634342>
- [30] Mike Sinclair, Eyal Ofek, Mar Gonzalez-Franco, and Christian Holz. 2019. CapstanCrunch: A Haptic VR Controller with User-supplied Force Feedback. In *Proceedings of the 32nd Annual ACM Symposium on User Interface Software and Technology*. 815–829.
- [31] Evan Strasnick, Christian Holz, Eyal Ofek, Mike Sinclair, and Hrvoje Benko. 2018. Haptic links: Bimanual haptics for virtual reality using variable stiffness actuation. In *Proceedings of the 2018 CHI Conference on Human Factors in Computing Systems*. 1–12.
- [32] Yuqian Sun, Shigeo Yoshida, Takuji Narumi, and Michitaka Hirose. 2019. PaCaPa: A Handheld VR Device for Rendering Size, Shape, and Stiffness of Virtual Objects in Tool-Based Interactions. In *Proceedings of the 2019 CHI Conference on Human Factors in Computing Systems (CHI '19)*. Association for Computing Machinery, New York, NY, USA, Article Paper 452, 12 pages. DOI: <http://dx.doi.org/10.1145/3290605.3300682>
- [33] Colin Swindells, Alex Unden, and Tao Sang. 2003. TorqueBAR: an ungrounded haptic feedback device. In *Proceedings of the 5th international conference on Multimodal interfaces*. 52–59.
- [34] Shan-Yuan Teng, Tzu-Sheng Kuo, Chi Wang, Chi-huan Chiang, Da-Yuan Huang, Liwei Chan, and Bing-Yu Chen. 2018. PuPoP: Pop-up Prop on Palm for Virtual Reality. In *Proceedings of the 31st Annual ACM Symposium on User Interface Software and Technology (UIST '18)*. Association for Computing Machinery, New York, NY, USA, 5–17. DOI: <http://dx.doi.org/10.1145/3242587.3242628>
- [35] Wouter M Bergmann Tiest and Astrid ML Kappers. 2009. Cues for haptic perception of compliance. *IEEE transactions on haptics* 2, 4 (2009), 189–199.
- [36] Yoshimasa Tokuyama, RPC Janaka Rajapakse, Yuji Nakazawa, and Kouichi Konno. 2009. Torque display method for free-form deformation with haptic device. In *2009 ICCAS-SICE*. IEEE, 3803–3808.
- [37] Cui Tong, Aiguo Song, and Wu Juan. 2007. A mass-spring model for haptic display of flexible object global deformation. In *2007 International Conference on Mechatronics and Automation*. IEEE, 2753–2757.
- [38] Hsin-Ruey Tsai and Bing-Yu Chen. 2019. ElastImpact: 2.5D Multilevel Instant Impact Using Elasticity on Head-Mounted Displays. In *Proceedings of the 32nd Annual ACM Symposium on User Interface Software and Technology (UIST '19)*. Association for Computing Machinery, New York, NY, USA, 429–437. DOI: <http://dx.doi.org/10.1145/3332165.3347931>
- [39] Hsin-Ruey Tsai, Ching-Wen Hung, Tzu-Chun Wu, and Bing-Yu Chen. 2020. ElastOscillation: 3D Multilevel Force Feedback for Damped Oscillation on VR Controllers. In *Proceedings of the 2020 CHI Conference on Human Factors in Computing Systems (CHI '20)*. Association for Computing Machinery, New York, NY, USA, 1–12. DOI: <http://dx.doi.org/10.1145/3313831.3376408>
- [40] Hsin-Ruey Tsai, Jun Rekimoto, and Bing-Yu Chen. 2019. ElasticVR: Providing Multilevel Continuously-Changing Resistive Force and Instant Impact Using Elasticity for VR. In *Proceedings of the 2019 CHI Conference on Human Factors in Computing Systems*. 1–10.
- [41] C. Wang, C. Hsieh, N. Yu, A. Bianchi, and L. Chan. 2019. HapticSphere: Physical Support To Enable Precision Touch Interaction in Mobile Mixed-Reality. In *2019 IEEE Conference on Virtual Reality and 3D User Interfaces (VR)*. 331–339.
- [42] Takeshi Yamamoto and Koichi Hirota. 2015. Recognition of weight through shaking interaction. In *2015 IEEE World Haptics Conference (WHC)*. IEEE, 451–456.

- [43] Andre Zenner and Antonio Krüger. 2017. Shifty: A weight-shifting dynamic passive haptic proxy to enhance object perception in virtual reality. *IEEE transactions on visualization and computer graphics* 23, 4 (2017), 1285–1294.
- [44] André Zenner and Antonio Krüger. 2019. Drag: on: A Virtual Reality Controller Providing Haptic Feedback Based on Drag and Weight Shift. In *Proceedings of the 2019 CHI Conference on Human Factors in Computing Systems*. 1–12.